Appl. Phys. B (2015) 120:601–607
DOI 10.1007/s00340-015-6171-4

Applied Physics B
Lasers and Optics

Thermo-optic properties of Yb:Lu_2O_3 single crystals

P. A. Loiko[1] · K. V. Yumashev[1] · R. Schödel[2] · M. Peltz[3] · C. Liebald[3] · X. Mateos[4] · B. Deppe[5,6] · C. Kränkel[5,6]

Received: 11 May 2015 / Accepted: 7 July 2015 / Published online: 19 July 2015
© Springer-Verlag Berlin Heidelberg 2015

Abstract A detailed study of thermo-optic properties of 1.5 at.% Yb:Lu_2O_3 single crystal is performed. Thermo-optic dispersion formulas are derived for dn/dT coefficient and thermal coefficient of the optical path. At the wavelength of 1.03 μm, dn/dT = 5.8 × 10^{-6} K^{-1}. High-precision temperature-dependent measurements of the thermal expansion coefficient α are performed. At the room temperature (RT), α = 5.880 ± 0.014 × 10^{-6} K^{-1}. Temperature dependence of the bandgap is analyzed, yielding RT value of E_g = 5.15 eV and dE_g/dT = –3.7 × 10^{-4} eV/K. Sensitivity factor of the thermal lens is calculated for a diode-pumped Yb:Lu_2O_3 crystal versus the pump spot radius and crystal temperature.

1 Introduction

The very high melting point of 2450 °C [1] imposes serious challenges for the growth of the cubic sesquioxide lutetia (Lu_2O_3). Initial growth attempts of sesquioxides utilized the Verneuil method [2, 3] or the floating zone technique [4]. The resulting mm-size crystals of low quality were utilized for the initial determination of the optical and thermo-mechanical properties of these materials and even allowed for first flash-lamp-pumped laser experiments [5]. Afterward, different growth methods such as the laser-heated pedestal growth (LHPG) [6], the micro-pulling down technique [7] and the Czochralski technique [8] were applied, but still the crystals were limited in size and quality. It was not before 2008 that by the optimization of the heat exchanger method [9] the growth of cm-scale single-crystalline sesquioxides with excellent optical quality became possible [10]. In the following years, in particular cubic sesquioxide host material lutetia (Lu_2O_3) has been shown to be an excellent host material for various rare earth ions [11]. Efficient and high-power laser operation has been demonstrated utilizing various laser ions such as Yb^{3+} [12, 13] at 1 μm, Tm^{3+} [14] and Ho^{3+} [15] at 2 μm as well as Er^{3+} at 3 μm [16].

These outstanding laser results obtained in the past motivate a reexamination of the thermo-optic properties of Lu_2O_3 that affect the parameters of the thermal lens. The lens-like behavior is related with three main effects, namely temperature dependence of the refractive index (expressed by the thermo-optic coefficient, dn/dT), end-bulging related to the thermal expansion coefficient α, as well as photoelastic effect that is responsible for the lens astigmatism and birefringence losses. Under the plane stress approximation (that refers to the diode pumping case), first two terms are dominant [17]. Thus, the knowledge of dn/dT and α values as well as their combination, called thermal coefficient of the optical path (TCOP) [18], is crucial for the determination of the thermal lens parameters and, hence, the cavity design. Indeed, non-compensated thermal lens can lead to

✉ P. A. Loiko
kinetic@tut.by

1 Center for Optical Materials and Technologies, Belarusian National Technical University, 65/17 Nezavisimosti Ave., 220013 Minsk, Belarus

2 PTB, Bundesallee 100, 38116 Brunswick, Germany

3 FEE GmbH, Struthstr. 2, 55743 Idar-Oberstein, Germany

4 Física i Cristallografia de Materials i Nanomaterials (FiCMA-FiCNA), Universitat Rovira i Virgili (URV), Campus Sescelades, c/Marcellí Domingo, s/n., 43007 Tarragona, Spain

5 Institut für Laser-Physik, Universität Hamburg, Luruper Chaussee 149, 22761 Hamburg, Germany

6 The Hamburg Centre for Ultrafast Imaging, Luruper Chaussee 149, 22761 Hamburg, Germany

the cavity instability, distortion of the output laser beam as well as rapid increase in the M^2 parameter, violation of the mode-matching conditions and even laser ceasing [17].

Previously, a lot of attention was paid to the study of dn/dT and TCOP coefficients for sesquioxide ceramics [19–21] that is, however, not equivalent to the bulk single crystals in terms of its thermo-optic behavior. In particular, comprehensive temperature-dependent measurements for pure and Yb-doped Lu_2O_3 ceramics were reported by Cardinally et al. [19], however, without any dispersion analysis. In contrast, there are only few investigations of bulk crystals, due to the above-mentioned problem of the growth of large-volume crystals typically required for such measurements. In particular, Zelmon et al. [22] recently reported on the dispersion of dn/dT values for pure Lu_2O_3 by a standard minimum deviation method, however, without the determination of α and TCOP values. In the present paper, we report on a comprehensive study of dispersion of dn/dT and TCOP coefficients yielding useful thermo-optic dispersion formulas, as well as precise measurements of thermal expansion ones. Temperature dependence of the thermal lens parameters is also discussed.

2 Experimental

The 1.5 at.% doped Yb:Lu_2O_3 crystals used for the experiments were grown from 5 N starting materials. The starting materials were heated up in an 80-mm-diameter rhenium crucible which was covered by a lid with a hole to monitor the melt temperature by a W–Re thermocouple. Thermal insulation of the crucible was provided by ZrO_2 felts and Al_2O_3 ceramics. As growth atmosphere, a mixture of 95 % N_2 and 5 % H_2 at a flow rate of 30 l/h was used. After heating the crystal to the melting point, the crucible was cooled down within 40 h. Despite the absence of a cooling gas flow usually applied during the growth by the heat exchanger method [10], the large size of the crucible enabled the growth of cm-scale monocrystalline regions with excellent optical quality. From these regions, two rectangular samples with dimensions of 9.6 × 4.9 × 4.9 mm^3 were extracted. The small apertures were polished to laser quality with a parallelism of the two apertures of 24" (sample 1) and 2" (sample 2).

For the thermo-optic study of Yb:Lu_2O_3 crystal, we used the laser beam deviation method for media with a linear thermal gradient [23]. The thermo-optic coefficient dn/dT and the thermal coefficient of the optical path (TCOP) were determined around the room temperature (RT) with a precision of ~0.2 × 10^{-6} K^{-1} using sample 1. The thermal gradient (~50 K between the "hot" and "cold" surfaces, or ~10 K/mm) was applied perpendicularly to the light propagation direction. The experimental details can be found elsewhere [24]. The same sample was used for the determination of thermal expansion coefficient α with a horizontal dilatometer Netzsch 402 PC, providing a precision of ~0.1 × 10^{-6} K^{-1}. The measurements were performed in the temperature range 360–470 K.

Alternatively, thermal expansion coefficient was measured in Physikalisch-Technische Bundesanstalt (PTB) with PTB's Ultra Precision Interferometer (UPI) described in [25]. For this, sample 2 with the same dimensions and specifications but a slightly better parallelism was used. The length of the sample was measured at different temperatures by high-resolution phase stepping interferometry [26–28]. Two J_2-stabilized lasers at 532 and 633 nm were used subsequently for this purpose, and the results were averaged. All measurements were performed under vacuum conditions. The total uncertainty of the length measurements in this method is 1.0 nm. The temperature near the sample was determined with an estimated uncertainty of 6 mK at RT by thermocouples placed right and left to the sample. The length of the sample was monitored over a total duration of 15 days where the temperature was decreased in steps of 5 K every 24 h.

The extraction of the coefficient α and its uncertainty from the measurements was made as described in detail in [29]. A least square fitting was performed so that a specific gauge block length as a function of the temperature is described by a polynomial fit of the degree n:

$$l^{(n)} = a_0 + a_1\vartheta + a_2\vartheta^2 + \cdots + a_n\vartheta^n, \tag{1}$$

where $\vartheta = T - T_0$ and T_0 is set to 303 K. From these data, the value for α in the temperature interval between 283 and 323 K was calculated according to:

$$\alpha^n = \frac{1}{l^{(n)}} \cdot \frac{\mathrm{d}l^{(n)}}{\mathrm{d}T} \quad \text{using } n = 3. \tag{2}$$

The temperature-dependent position of the UV absorption edge of a third Yb:Lu_2O_3 crystal was measured using Varian CARY 5000 spectrophotometer equipped with an Oxford Instruments cryostat (SU 12 model) with closed-cycle helium gas flow in the temperature range between 223 and 313 K. For these experiments, a 500-μm-thin polished plate was used.

3 Results and discussion

The values of the thermal expansion coefficient α for Yb:Lu_2O_3 are summarized in Fig. 1. Here open and filled circles represent data obtained with the dilatometry and interferometry, respectively. The temperature dependence of the value for α is clearly nonlinear. A profound change is observed only for the first 100 K above RT; the corresponding temperature derivative of the thermal expansion

coefficient $d\alpha/dT$ is $+0.8 \times 10^{-8}$ K^{-2}. At higher temperatures, a kind of saturation is observed. To fit the temperature dependence, a polynomial law was used:

$$\alpha(T) = A_0 + A_1 T + A_2 T^2 + A_3 T^3. \quad (3)$$

The best-fitting values for the constants A_i are $A_0 = -1.96 \times 10^{-6}$ K^{-1}, $A_1 = 4.51 \times 10^{-8}$ K^{-2}, $A_2 = -7.30 \times 10^{-11}$ K^{-3} and $A_3 = 3.68 \times 10^{-14}$ K^{-3}.

The inset in Fig. 1 shows a more detailed analysis of the dependence of $\alpha(T)$ for the temperature interval 283–323 K. The error bars represent the total uncertainty that takes into account the arbitrariness of the polynomial's order of 3, see [29]. Thus, we can state that the value for α at RT (293 K) is $(5.880 \pm 0.014) \times 10^{-6}$ K^{-1}. This value is in significant deviation to the value of $\alpha = 8.9 \times 10^{-6}$ K^{-1} previously reported in [30]. We attribute this to the inferior quality and small size of previously available samples.

Measured thermo-optic coefficients dn/dT for Yb:Lu_2O_3 crystal are shown in Fig. 2a. To fit their wavelength dependence (dispersion), the theory of the temperature dependence of the refractive index was involved [31]. It includes the impact of the volumetric thermal expansion (expressed by $\alpha_{vol} = 3\alpha$ value), as well as the temperature dependence of the bandgap E_g (expressed by a constant dE_g/dT). The expression for dn/dT is then:

$$\frac{dn}{dT}(\lambda) = -\alpha_{vol}\frac{(n_\infty^2 - 1)}{2n(\lambda)}\frac{\lambda^2}{\lambda^2 - \lambda_g^2} + \frac{1}{E_g}\left|\frac{dE_g}{dT}\right|\frac{(n_\infty^2 - 1)}{2n(\lambda)}\left(\frac{\lambda^2}{\lambda^2 - \lambda_g^2}\right)^2. \quad (4)$$

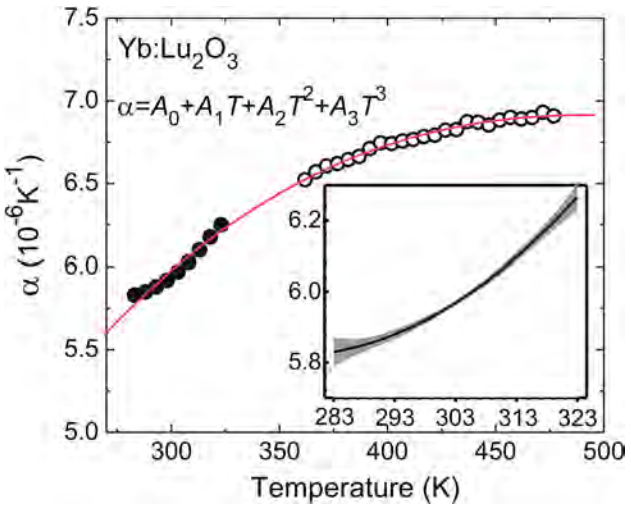

Fig. 1 Temperature dependence of thermal expansion coefficient α for Yb:Lu_2O_3: *open* and *filled circles* represent data obtained with the dilatometry and interferometry, respectively, *curve* is their fitting with a polynomial law, Eq. (3). *Inset* shows detailed analysis of interferometric data: *gray region* is the uncertainty estimation; *solid curve* corresponds to the experimental data

Here, n_∞ is the refractive index of the crystal in the long-wavelength limit and λ_g is the wavelength corresponding to the bandgap energy, $\lambda_g(\mu m) = 1.2396/E_g$ (eV). The Sellmeier equation for the refractive index was taken from [22]. The best-fitting values are $\alpha_{vol} = 18 \pm 2 \times 10^{-6}$ K^{-1}, $E_g = 5.2 \pm 0.1$ eV and $dE_g/dT = -1.8 \pm 0.5 \times 10^{-4}$ eV/K. The fitting was extended up to ~2 μm, the region of interest for Tm- and Ho-doped Lu_2O_3 crystals [14, 15]. The thermo-optic coefficients for Yb:Lu_2O_3 are positive for the whole spectral range between 0.4 and 2 μm. This is mainly caused by a relatively strong temperature dependence of the bandgap that has a positive contribution to the "overall" dn/dT value in Eq. (4). In contrast, volumetric thermal expansion tends to decrease the refractive index with temperature. However, for Yb:Lu_2O_3 the latter is relatively weak and thus cannot change the sign of dn/dT. At the typical Yb emission wavelength of 1030 nm, the value for dn/dT is 5.8×10^{-6} K^{-1}. The dispersion of the thermo-optic coefficient in Yb:Lu_2O_3 is more pronounced in the short-wavelength range close to the UV absorption edge, while in the near-IR it remains nearly unchanged.

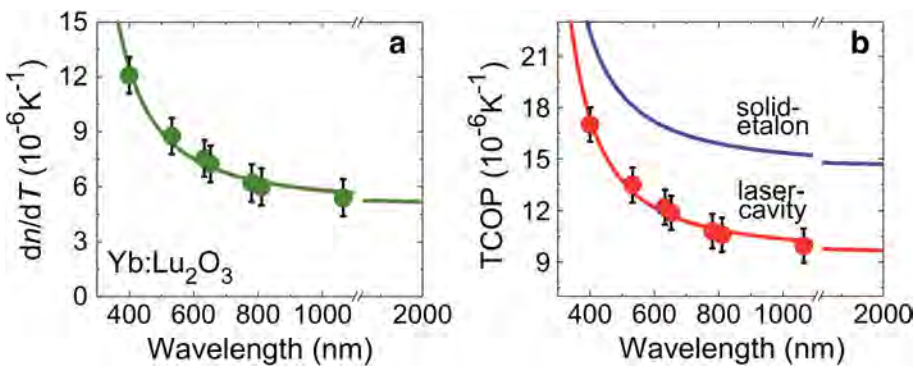

Fig. 2 Dispersion of the thermo-optic coefficient dn/dT and thermal coefficient of the optical path (TCOP) for Yb:Lu_2O_3 crystal: *points* are the experimental data, and *curves* are their fitting with Eq. (4)

Table 1 Expansion coefficients in the thermo-optic dispersion formulas for Yb:Lu_2O_3 crystal, Eq. (5)

Parameter	Expansion coefficients			
	B_0	B_1 (μm^2)	B_2 (μm^4)	B_3 (μm^6)
dn/dT	4.97	0.834	0.0051	0.0085
$W_1 = \mathrm{d}n/\mathrm{d}T + (n-1)\alpha$	9.44	0.915	0.0009	0.0088
$W_2 = \mathrm{d}n/\mathrm{d}T + n\alpha$	14.44	0.915	0.0008	0.0088

To describe the thermo-optic dispersion in a simple analytical form, we used the following formula [32]:

$$\frac{\mathrm{d}n}{\mathrm{d}T}(\lambda) = B_0 + \frac{B_1}{\lambda^2} + \frac{B_2}{\lambda^4} + \frac{B_3}{\lambda^6}\left[10^{-6}\,\mathrm{K}^{-1}\right]. \quad (5)$$

Here, the light wavelength λ is expressed in μm. The expansion constants B_i are summarized in Table 1; B_0 corresponds to the dn/dT value in the long-wavelength limit and the constants B_1, B_2 and B_3 describe its dispersion close to the UV absorption edge. The deviation between the data calculated with Eqs. (4) and (5) is within 5 %.

For a uniformly heated crystal, both temperature dependence of the refractive index and thermal expansion play a role in the "overall" change in the optical path length. Both contributions are summarized in a so-called thermal coefficient of the optical path (TCOP) [33]:

$$W_1 = \mathrm{d}n/\mathrm{d}T + (n-1)\alpha, \quad (6a)$$

$$W_2 = \mathrm{d}n/\mathrm{d}T + n\alpha. \quad (6b)$$

These two equations correspond to different crystal configurations, called "laser cavity" (W_1) and "solid-etalon" (W_2). In the first case, the light is considered to propagate through the crystal and surrounding air. In the second case, light propagation is considered solely inside the crystal (the case of microchip setup). The laser beam deviation method allowed us to measure the values for W_1 directly, see points in Fig. 2b. In addition, using thermo-optic, Eq. (5), and Sellmeier [22] equations, it is straightforward to calculate the dispersion of both W constants, as shown in Fig. 2b.

The dispersion of TCOP values follows the behavior of the refractive index and the thermo-optic coefficient. At a wavelength of 1030 nm, $W_1 = 10.3 \times 10^{-6}$ K^{-1} and $W_2 = 15.3 \times 10^{-6}$ K^{-1}. The analytical expressions for both TCOP values were derived using an expression similar to Eq. (5). The resulting B_i constants for the TCOP are summarized in Table 1. The positive values of the TCOP value for the "solid-etalon" configuration indicate the principal possibility of microchip laser operation [34] with Yb:Lu_2O_3. This is related to the resulting positive thermal lens that provides the desired stabilization of the laser mode in the plano–plano cavity (that would otherwise be unstable) [35].

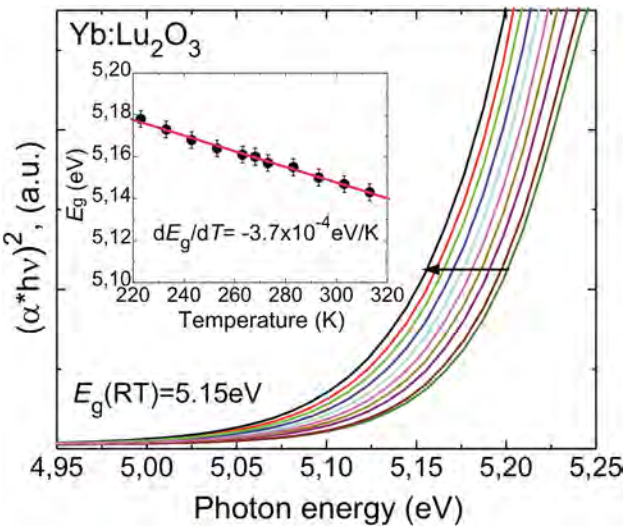

Fig. 3 Temperature-dependent Tauc plot for Yb:Lu_2O_3 crystal; the spectra are measured from 223 to 313 K through 10 K (following the *arrow*); and *inset* represents obtained E_g values versus crystal temperature

Previously, the dn/dT for Lu_2O_3 was measured by a conventional minimum deviation method [22] (TCOP values were not reported). At RT, it was found to be ~7.2 × 10^{-6} K^{-1} around ~1 μm. This value is slightly larger than in the present study. Cardinalli et al. [19] determined the RT dn/dT value for 1 at.% Yb:Lu_2O_3 ceramics to be 8.1 × 10^{-6} K^{-1} at 633 nm, a value which is in good agreement with our result, 7.5 × 10^{-6} K^{-1}.

Also the fitting parameters of the thermo-optic dispersion formulas, α_{vol} is in good agreement with the expected value $\alpha_{vol} = 3\alpha = 17.64 \times 10^{-6}$ K^{-1} resulting from the measured RT thermal expansion coefficient. For conclusions regarding the E_g and dE_g/dT values, we performed temperature-dependent measurements of the UV absorption edge in Yb:Lu_2O_3. For this, the absorption was measured versus the photon energy E. Then, the spectrum was recalculated as $(\alpha_{abs}E)^2$; the approach that is known as Tauc plot. According to the Urbach's rule for band tails and assuming that the ultraviolet absorption is due to direct dipole-allowed interband transitions, the extrapolation of the linear part of such a plot to zero yields the bandgap energy E_g.

The results are shown in Fig. 3. The lines correspond to the Tauc plots for the temperatures between 223 and 313 K; the inset represents the obtained E_g values as well as the evaluation of the value for dE_g/dT. The RT value of E_g for Yb:Lu_2O_3 crystal is 5.15 eV (λ_g = 241 nm) that is again consistent with the fitting data. For an undoped Lu_2O_3 crystal studied in a similar manner, the resulting value was E_g = 5.41 eV (λ_g = 220 nm), so 1 at.% Yb doping appears to result in a substantial variation of the band structure. Ordin et al. [36] recently reported E_g = 5.5 eV

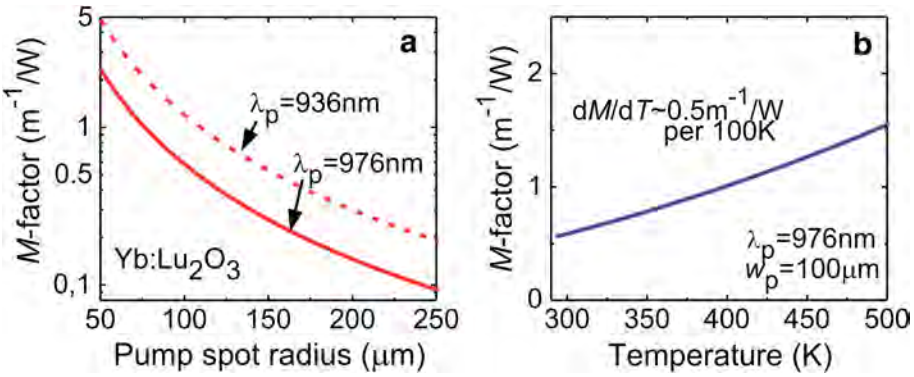

Fig. 4 Sensitivity factors of the thermal lens M for Yb:Lu_2O_3 crystal calculated with Eqs. (7) and (8) versus the pump spot radius (**a**) and crystal temperature (**b**)

for Lu_2O_3 that agrees with our data. The value of dE_g/dT is $-3.7 \pm 0.5 \times 10^{-4}$ eV/K. This is higher than the value obtained in the present paper from fitting. A similar deviation was observed previously for double tungstates (DTs) [31]. It was referred to the impact of defect and impurity states located close to the band tails. Indeed, the growth of Yb:Lu_2O_3 induces color centers that cause dark, red or blue crystal coloration. A subsequent heat treatment (annealing) in air typically allows for a rediffusion of oxygen into the crystal removing the color centers [37]. For the crystals examined in this report, this process may have been non-complete as indicated by a light yellowish color of the samples.

To calculate the optical (refractive) power of the thermal lens D in an efficient diode-pumped Yb:Lu_2O_3 crystal, the following formula can be applied [17]:

$$D = \frac{\eta_h P_{abs}}{2\pi w_p^2 \kappa}\left[\frac{dn}{dT} + (n-1)(1+\nu)\alpha\right]. \quad (7)$$

Here P_{abs} is the absorbed pump power, η_h is the fractional heat load, i.e., the fraction of P_{abs} that is dissipated as heat, w_p is the pump spot radius (a "top-hat" beam profile is considered as a good approximation for the output of fiber-coupled laser diodes), and κ is the thermal conductivity. The η_h for Yb:Lu_2O_3 with high expected luminescence quantum yield [11] can be estimated to equal the Stokes shift, $1-\lambda_p/\lambda_f$, where λ_p is the pump wavelength and λ_f is the average fluorescence emission wavelength [38]. For Yb:Lu_2O_3, we determined λ_f to be 1013.5 nm. The expression in squared brackets is called "generalized" thermo-optic coefficient χ, $\nu = 0.288$ is the Poisson ratio [39]. In the expression for χ, we omitted the so-called photoelastic term that is responsible for the astigmatism of the lens. This is because the photoelastic constants required for its calculation are not reported for Lu_2O_3. In general, the contribution of this term to the "overall" χ value in the case of diode pumping is low (e.g., <5 % for Yb:YAG [17]).

As can be seen from Eq. (7), the optical power of the thermal lens depends on the pump power level. To express this feature, so-called sensitivity factor is introduced [40]:

$$M = \frac{dD}{dP_{abs}}. \quad (8)$$

It shows the change in the optical power due to 1 W variation of the absorbed pump power. The values of sensitivity factors of the thermal lens for Yb:Lu_2O_3 crystals are plotted in Fig. 4a versus the pump spot radius (for two widely used pump wavelengths, λ_p = 936 and 976 nm). For w_p = 100 μm, the resulting sensitivity factors are $M_{936nm} = 1.19 \pm 0.05$ m^{-1}/W and $M_{976nm} = 0.58 \pm 0.05$ m^{-1}/W, respectively. The deviation is mainly caused by the lower Stokes efficiency and thus higher heat load when pumping at 936 nm. Thus, although the value $\chi \sim 12.6 \times 10^{-6}$ K^{-1} is far from zero for Yb:Lu_2O_3 at ~1 μm, the thermal lensing in this crystal is relatively weak. It is nearly 2.2 times weaker than for Yb:YAG for the same w_p [17]. This results mainly from the high thermal conductivity of Yb:Lu_2O_3 of κ = 12.3 Wm^{-1}/K for 1 at.% doping with Yb [12].

Optical pumping of a laser crystal results in a complex temperature distribution in its volume responsible for the thermal lensing effect. On the other hand, this temperature rise leads to a variation of the material parameters like dn/dT, α and κ. Thus, this will impact the value of sensitivity factor M. The question here is the definition of the crystal temperature used in the calculation of the material parameters. As the laser mode within the laser crystal has a radius of few hundreds of μm, an averaged temperature can be easily defined for this small volume. The values of temperature derivatives of dn/dT, α and κ for Lu_2O_3, as well as their RT values, are listed in Table 2. Calculated M factors for λ_p = 976 nm and w_p = 100 μm vs. the crystal temperature are shown in Fig. 4b. The temperature rise of 200 K – considered to be above the limit for efficient diode-pumped bulk laser operation in ground state lasers based on Yb^{3+}, Tm^{3+}

Table 2 Temperature dependence of main thermal and thermo-optic parameters of Lu_2O_3

Parameter	Notation	RT value	Ref.	Notation[a]	Above RT	Ref.
Thermo-optic coefficient	dn/dT	5.8×10^{-6} K^{-1} at 1.03 μm	This paper	d^2n/dT^2	$+2.6 \times 10^{-8}$ K^{-2} at 1.03 μm	[22]
Thermal expansion	α	5.83×10^{-6} K^{-1}	This paper	$d\alpha/dT$	$+0.8 \times 10^{-8}$ K^{-2}	This paper
Thermal conductivity	κ	12.3 W/mK	[12]	$d\kappa/dT$	−0.03 W/mK^2	[41]

[a] Notation for temperature derivative

or Ho^{3+}—results in a more than two times enhancement of the optical power of the thermal lens. The dM/dT parameter is then ~0.5 m^{-1}/W per 100 K.

4 Conclusions

For the first time, the coefficient of thermal expansion (CTE) α was determined for macroscopic samples of Lu_2O_3. The measurements performed at PTB's Ultra Precision Interferometer (UPI) indicate a value of α $(5.880 \pm 0.014) \times 10^{-6}$ K^{-1} at room temperature (293 K). This value is about 50 % lower than previously reported values. This refinement is of great importance for further laser experiments with rare-earth-doped sesquioxides when it comes to the choice of CTE-matched heat sinks or the cavity design.

For the latter purpose, we furthermore determined the dispersion of the thermo-optic coefficient, dn/dT, as well as the thermal coefficient of the optical path (TCOP). In this way, the thermo-optic dispersion formulas for the spectral range between 0.4 and 2 μm were determined. At the typical Yb wavelength of 1.03 μm, the dn/dT was determined to be 5.8×10^{-6} K^{-1}. The physical reasons for positive values of dn/dT in Yb:Lu_2O_3 are analyzed, and the results are supported by the CTE measurements as well as the determination of the electronic bandgap energy ($E_g = 5.15$ eV at RT). The impact of material parameters on the thermal lensing properties in Yb:Lu_2O_3 crystal is discussed.

References

1. J.-P. Coutures, R. Verges, M. Foex, Rev. Int. Hautes Temp. Réfract. **12**, 181 (1975)
2. C. Bárta, F. Petru, B. Hájek, Naturwissenschaften **45**, 36 (1958)
3. A.C. Pastor, R.C. Pastor, Mater. Res. Bull. **2**, 555 (1967)
4. D.B. Gasson, D.S. Cockayne, J. Mater. Sci. **5**, 100 (1970)
5. R.H. Hoskins, B.H. Soffer, Appl. Phys. Lett. **4**, 22 (1964)
6. B.M. Tissue, L. Lu, L. Ma, W. Jia, M.L. Norton, W.M. Yen, J. Cryst. Growth **109**, 323 (1991)
7. J.H. Mun, A. Jouini, A. Novoselov, Y. Guyot, A. Yoshikawa, H. Ohta, H. Shibata, Y. Waseda, G. Boulon, T. Fukuda, Opt. Mater. **29**, 1390 (2007)
8. L. Fornasiero, E. Mix, K. Petermann, G. Huber, Cryst. Res. Technol. **34**, 255 (1999)
9. F. Schmid, D. Viechnicki, J. Am. Ceram. Soc. **53**, 528 (1970)
10. R. Peters, C. Kränkel, K. Petermann, G. Huber, J. Cryst. Growth **310**, 1934 (2008)
11. C. Kränkel, IEEE J. Sel. Top. Quantum Electron. **21**(1), 1602013 (2015)
12. R. Peters, C. Kränkel, S.T. Fredrich-Thornton, K. Beil, K. Petermann, G. Huber, O.H. Heckl, C.R.E. Baer, C.J. Saraceno, T. Südmeyer, U. Keller, Appl. Phys. B **102**, 509 (2011)
13. C.R.E. Baer, C. Kränkel, C.J. Saraceno, O.H. Heckl, M. Golling, R. Peters, K. Petermann, T. Südmeyer, G. Huber, U. Keller, Opt. Lett. **35**, 2296 (2010)
14. P. Koopmann, S. Lamrini, K. Scholle, P. Fuhrberg, K. Petermann, G. Huber, Opt. Lett. **36**, 948 (2011)
15. P. Koopmann, S. Lamrini, K. Scholle, M. Schäfer, P. Fuhrberg, G. Huber, Opt. Express **21**, 3926 (2013)
16. T. Li, K. Beil, C. Kränkel, G. Huber, Opt. Lett. **37**, 2568 (2012)
17. S. Chenais, F. Druon, S. Forget, F. Balembois, P. Georges, Prog. Quantum Electron. **30**, 89 (2006)
18. S. Biswal, S.P. O'Connor, S.R. Bowman, Appl. Opt. **44**, 3093 (2005)
19. V. Cardinali, E. Marmois, B. Le Garrec, G. Bourdet, Opt. Mater. **34**, 990 (2012)
20. T.Y. Fan, IEEE J. Sel. Top. Quantum Electron. **13**, 448 (2007)
21. I.L. Snetkov, D.E. Silin, O.V. Palashov, E.A. Khazanov, H. Yagi, T. Yanagitani, H. Yoneda, A. Shirakawa, K. Ueda, A.A. Kaminskii, Opt. Express **21**, 21254 (2013)
22. D.E. Zelmon, J.M. Northridge, N.D. Haynes, D. Perlov, K. Petermann, Appl. Opt. **52**, 3824 (2013)
23. S. Vatnik, M.C. Pujol, J.J. Carvajal, X. Mateos, M. Aguiló, F. Díaz, V. Petrov, Appl. Phys. B **95**, 653 (2009)
24. P. Loiko, F. Druon, P. Georges, B. Viana, K. Yumashev, Opt. Mater. Express **4**, 2241 (2014)
25. R. Schödel, A. Walkov, M. Zenker, G. Bartl, R. Meeß, D. Hagedorn, C. Gaiser, G. Thummes, S. Heltzel, Meas. Sci. Technol. **23**, 094004 (2012)
26. R. Schödel, Meas. Sci. Technol. **19**, 084003 (2008)
27. R. Schödel, A. Nicolaus, G. Bönsch, Appl. Opt. **41**, 55 (2002)
28. R. Schödel, G. Bönsch, Appl. Opt. **43**, 5738 (2004)
29. R. Schödel, Proc. SPIE **5879**, 1 (2005)
30. H. Bergman, *Gmelin Handbuch der Anorganischen Chemie, Seltenerdelemente, Teil C 1* (Springer, Berlin, 1974)
31. P.A. Loiko, K.V. Yumashev, N.V. Kuleshov, G.E. Rachkovskaya, A.A. Pavlyuk, Opt. Mater. **33**, 1688 (2011)
32. P.A. Loiko, X. Han, K.V. Yumashev, N.V. Kuleshov, M.D. Serrano, C. Cascales, C. Zaldo, Appl. Phys. B **111**, 279 (2013)
33. P.A. Loiko, K.V. Yumashev, N.V. Kuleshov, A.A. Pavlyuk, Appl. Phys. B **102**, 117 (2011)
34. J.J. Zayhowski, A. Mooradian, Opt. Lett. **14**, 24 (1989)
35. J.M. Serres, X. Mateos, P. Loiko, K. Yumashev, N. Kuleshov, V. Petrov, U. Griebner, M. Aguiló, F. Díaz, Opt. Lett. **39**, 4247 (2014)
36. S.V. Ordin, A.I. Shelykh, Semiconductors **44**, 558 (2010)
37. K. Petermann, L. Fornasiero, E. Mix, V. Peters, Opt. Mater. **19**, 67 (2002)

38. J. Körner, V. Jambunathan, J. Hein, R. Seifert, M. Loeser, M. Siebold, U. Schramm, P. Sikocinski, A. Lucianetti, T. Mocek, M.C. Kaluza, Appl. Phys. B **116**, 75 (2013)
39. M.J. Weber, *Handbook of Optical Materials* (CRC Press, New York, 2003)
40. P.A. Loiko, K.V. Yumashev, V.N. Matrosov, N.V. Kuleshov, Appl. Opt. **52**, 698 (2013)
41. P.H. Klein, W.J. Croft, J. Appl. Phys. **38**, 1603 (1967)